

Micro-architecture study of the normal odontoid with micro-computed tomography

Wei Wang, Zhijun Li, Yingna Qi, Lianxiang Chen, Ping Yi, Feng Yang, Xiangsheng Tang & Mingsheng Tan

To cite this article: Wei Wang, Zhijun Li, Yingna Qi, Lianxiang Chen, Ping Yi, Feng Yang, Xiangsheng Tang & Mingsheng Tan (2018): Micro-architecture study of the normal odontoid with micro-computed tomography, The Journal of Spinal Cord Medicine, DOI: [10.1080/10790268.2018.1519995](https://doi.org/10.1080/10790268.2018.1519995)

To link to this article: <https://doi.org/10.1080/10790268.2018.1519995>



Published online: 02 Oct 2018.



Submit your article to this journal [↗](#)



Article views: 7



View Crossmark data [↗](#)

Research Article

Micro-architecture study of the normal odontoid with micro-computed tomography

Wei Wang^{1,2†}, Zhijun Li^{3†}, Yingna Qi¹, Lianxiang Chen⁴, Ping Yi⁵, Feng Yang⁵, Xiangsheng Tang⁵, Mingsheng Tan⁵

¹Graduate School, Beijing University of Chinese Medicine, Beijing, People's Republic of China, ²Department of Emergency, Inner Mongolia People's Hospital, Hohhot, People's Republic of China, ³Human Anatomy Teaching and Research Section (Digital Medical Center), Inner Mongolia Medical University Basic Medical College, Hohhot, People's Republic of China, ⁴Department of Hematology, Affiliated Hospital of Inner Mongolia Medical University, Hohhot, People's Republic of China, ⁵Department of Spine Surgery, China–Japan Friendship Hospital, Beijing, People's Republic of China

Introduction: Odontoid fractures easily lead to instability, causing spinal cord injury. The aim of this study was to measure and analyze the micro-architecture and morphometric parameters of the normal odontoid with high-resolution three-dimensional (3D) micro-computed tomography (micro-CT).

Methods: Micro-CT scans were obtained from five normal odontoid processes. The scanned data were reconstructed with micro-CT software, and the nutrient foramina and the ossification center of the base of the odontoid were revealed. The trabeculae of the odontoid were measured and divided into four parts to obtain the volume fraction of regions of interest.

Results: High-resolution 3D images of the micro-structures' parameters were obtained from the odontoid using micro-CT software. The images demonstrated sponge-like trabecular bone, with the trabeculae showing a complex, net-like micro-construction. The subchondral bone plate was of lamella-like, compact construction and extended and transformed into a net-like structure with rod-shaped trabeculae arranged radially in all directions. There was a statistically significant difference in the volume fraction compared with the region of interest in the fourth part of the trabeculae and the first part of the odontoid ($P < 0.05$). The nutrient foramina and the ossification center of the odontoid were also observed.

Conclusions: It is feasible to use high-resolution 3D micro-CT to evaluate the micro-architecture of the normal odontoid. Other studies can benefit from use of the micro-CT images, such as finite element evaluations.

Keywords: Axis, Odontoid, Micro-architecture, Micro-computed tomography

Introduction

The atlantoaxial complex, the keystone of the cervical spine, is located at the craniocervical junction. The odontoid is the central structure which plays an important role in the rotational balance of the atlantoaxial complex. It is well known that the odontoid fracture which often leads to instability and spinal cord injuries is on account of many kinds of energy injuries. However, there exists certain difficulties in the treatment

because of the complex anatomy of the cranio-cervical junction.^{1–5} Most conventional computed tomography (CT) can facilitate early detection of the odontoid fracture. But most conventional CT images have been obtained using low-resolution imaging modalities, with detection levels insufficient for micro-structure analyses. Micro-CT is a non-destructive, high-resolution imaging modality capable of revealing the micro-architecture which can accurately discriminate the trabecular bone from cortical bone compartments of bone specimens. Recently, a three-dimensional (3D) imaging modality with spatial resolution in the micrometer range which is 100 times better than that of the conventional clinical CT has been applied to the analysis of skeletal structures, such as the spine or the dental fields and

Correspondence to: Mingsheng Tan, Department of Spine Surgery, China-Japan Friendship Hospital, Beijing 100029, People's Republic of China; Ph: +86 10 84205012. Email: cnwwzj@126.com

[†]Wei Wang and Zhijun Li contributed equally to this paper and share first authorship.

Color versions of one or more of the figures in the article can be found online at www.tandfonline.com/yscm.

femoral head.⁶⁻⁹ To date, however, no high-resolution studies of the normal odontoid have appeared in the literature. We therefore decided to study the odontoid using micro-CT, assessing its 3D micro-architecture in its entirety by analyzing its morphological characteristics. We then used the micro-CT software to analyze the parameters of the trabecular bone in selected areas of interest in an attempt to describe more accurately the characteristics of skeletal trabecular bone structure characteristics, to further study incidence of the odontoid fracture characteristics.¹⁰

Materials and methods

Bone specimen selection

The human bone specimens of Chinese origin in this study were obtained from the Department of Spine Surgery, China–Japan Friendship Hospital, Beijing, China. Conforming to the requirements of the experiment research by bone anthropology appraisal standards, we selected five normal-axis bone specimens from dried adult bone. Bone specimens with metabolic disorders or fracture were excluded via macroscopic and radiological evaluations. We finally selected five bone specimens (mean age 52 years, range 41–63 years). The Medical Ethics Committee of the China–Japan Friendship Hospital approved this study.

Micro-CT scanning

All bone specimens were scanned with a micro-CT system (Inveon PET/CT; Siemens, Erlangen, Germany) in high-resolution mode. For each specimen, scans were performed with source voltage 80 kVp, current 500 μ A, and exposure time 600 ms. Each specimen was scanned continuously with the slice thickness and an inter-slice distance of 1 pixel (pixel size 16.7 μ m, total image 1024 slices, maximum image data 2.8 G). Cross-sectional images were reconstructed

using micro-CT software (Inveon Research Workplace software, MultiModal 3D Visualization; Siemens, Erlangen, Germany). The CT analysis software was used to process structural parameters. The images, which were obtained automatically from the micro-CT system, were segmented using thresholding. Scanning generated a series of planar transverse gray-value images. All images were segmented to remove noise, and the same threshold was used to extract the bone phase. The bone volume fraction parameters were then calculated (Fig. 1).

Morphological and trabecular bone morphometric analysis

Slices were reconstructed, and the trabecular architecture was visualized in three dimensions with the micro-CT software. The structures were then quantified by examining the corresponding micro-CT cross-sectional images. For calculating trabecular bone parameters, a cuboid micro-CT region of interest (ROI, outline the area to be processed from the processed image in the form of boxes, circles, ellipses, irregular polygons, etc.) in the marrow cavity containing only trabecular bone was selected ($300 \times 300 \times 150$ pixel³; cuboid axis parallel to the odontoid axis), taking into account the trabecular bone quality. The ROI was selected using an artificial contouring method. The four ROIs of cubical trabeculae were in different parts of the odontoid: part I, tip of odontoid; part II, neck of the odontoid; part III, odontoid body; part IV, base of odontoid. The following bone volume fraction parameters of the ROI were then calculated: trabecular bone volume/total volume (BV/TV, %); bone surface area/bone volume (BS/BV, mm^{-1}); bone trabecular thickness (Tb.Th, mm); trabecular number (Tb.N, mm^{-1}); trabecular spacing (Tb.Sp, mm); trabecular pattern factor (Tb.Pf, mm^{-1}).⁵ The morphological characteristics of the

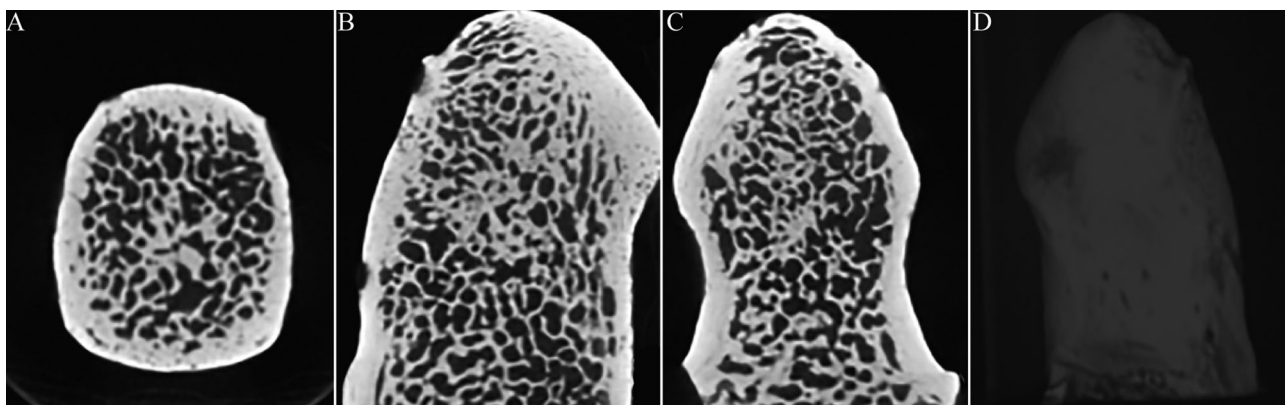


Figure 1 Micro-computed tomography (CT) images of the odontoid. (A: cross section, B: sagittal section, C: coronal section, D: three-dimensional, 3D).

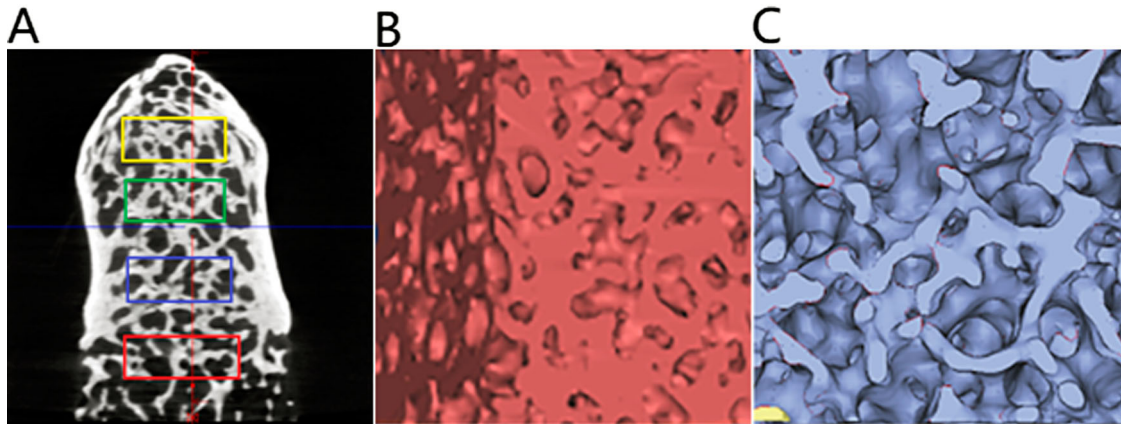


Figure 2 Region of interest (ROI) of the odontoid (A, the yellow rectangle represents part I, tip of odontoid. the green rectangle represents part II, neck of odontoid. the blue rectangle represents part III, odontoid body. the red rectangle represents part IV, base of odontoid); 3D reconstruction of cuboid trabeculae extracted from part I (B) and part IV (C) of the ROI.

nutrient foramen and the ossification center base structure were also analyzed.¹¹

Statistical analysis

Statistical analysis was performed using SPSS19.0 statistical software (IBM-SPSS Inc, Chicago, IL, USA). All values were expressed as the mean \pm SD. A value of $P < 0.05$ was considered to indicate statistical significance.

Results

Odontoid bone morphology

Micro-CT images revealed that the odontoid has multi-layered cortices, especially in the subchondral bone plate in the tip. This odontoid subchondral bone plate internal layer connects with rod-like trabeculae. The trabeculae maintain the marrow cavity of the odontoid from proximal to distal points. In coronal micro-CT images, the trabeculae ranges from a single-layer, internal subchondral bone plate to a multiple-layer, radially arranged structure. Micro-CT also revealed an ossification center forming a trabecular cavity whose micro-architecture was markedly different from that of normal trabecular bone. The 3D micro-CT images also revealed nutrient foramina in the superficial layers of the odontoid and into the subchondral bone.

Comparison of trabecular bone volume fractions

Other areas with trabecular bone had increased bone volume fractions, whereas part IV showed a decreased bone volume fraction. In the ROI of the marrow cavity, 3D morphometry showed that the BV/TV, Tb.Th and Tb.N of parts I had higher values than those of part IV, and the differences were statistically significant ($P < 0.05$). We also observed a negative correlation between BS/BV, Tb.Sp, and Tb.Pf in the odontoid. The BS/BV and Tb.Sp for parts I had lower values than those in part IV, and the differences were statistically significant ($P < 0.05$).

The Tb.Th of part I higher value than part III and the Tb.N of part I higher value than part II, the differences were statistically significant ($P < 0.05$). In addition, there were no significant differences in the bone volume fraction in parts II, and III ($P > 0.05$) (Fig. 2, Table 1).

Discussion

With our increasing aged populations worldwide, odontoid fractures pose an important axial fracture subtype. The Anderson system is commonly used to classify odontoid fractures into four types. Type II fractures occur at the base of the odontoid-body junction, they are common fractures in the geriatric population.^{12,13}

Table 1 Trabecular bone morphometric parameters measured with micro-CT ($n = 5$).

	BV/TV (%)	BS/BV (mm^{-1})	Tb.Th (mm)	Tb.N (mm^{-1})	Tb.Sp (mm)	Tb.Pf (mm^{-1})
Part I	0.60 ± 0.10	8.45 ± 1.48	$0.25 \pm 0.04^{\Delta}$	$2.84 \pm 0.28^{\#}$	0.16 ± 0.04	-3.21 ± 2.00
Part II	0.54 ± 0.08	9.58 ± 1.20	0.20 ± 0.02	2.43 ± 0.14	0.20 ± 0.04	-1.86 ± 1.66
Part III	0.48 ± 0.05	10.41 ± 1.46	0.18 ± 0.02	2.62 ± 0.24	0.22 ± 0.02	-0.84 ± 0.72
Part IV	$0.45 \pm 0.05^*$	$12.33 \pm 1.79^*$	$0.15 \pm 0.02^*$	$2.24 \pm 0.19^*$	$0.25 \pm 0.04^*$	$-0.44 \pm 0.78^*$

*vs part I; #vs part II; Δ vs part III, $P < 0.05$.

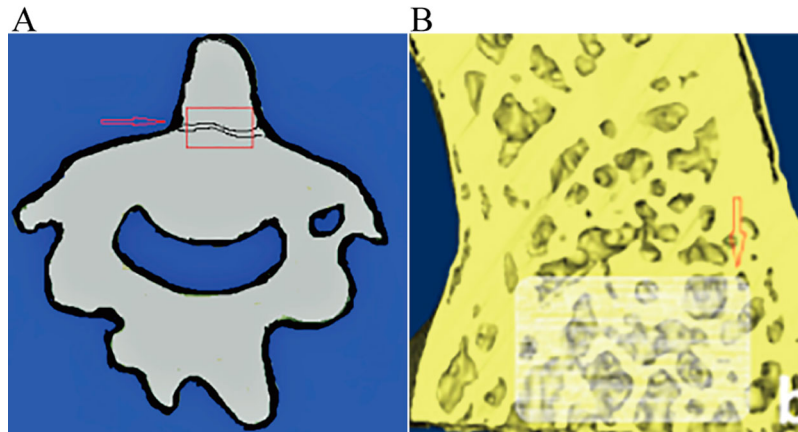


Figure 3 (A) Type II fracture; (B) 3D-Micro-computed tomography shows that low bone volume fractions represent weak points in the structure of part IV.

The influencing factors are complex and the mechanism is not yet clear, the anatomical specificity may be one of the important factors leading to type II fractures.

The bone volume fraction might contribute to maintaining the mechanical properties to resist the compressive stress of all kinds of energy fracture in trabecular bone. Measuring the volume fraction was of primary importance for evaluating trabecular micro-structure. The micro-CT system could be used to calculate the density of the selected 3D ROIs, and the bone volume fraction could be easily calculated from voxel-based 3D reconstructions.¹⁴ Low *et al.* studied the internal and external micro-architecture using high-resolution 3D micro-CT on the whole bone of the lunate, where they measured the trabecular bone volume fraction. They found that whole-bone high-resolution, 3D evaluation of the normal lunate could contribute to a better understanding of the micro-architectural changes occurring there. In the pathological trabecular bone of ROIs, the trabecular bone volume fraction showed significantly increased BV/TV, Tb.Th, and Tb.N and significantly decreased Tb.Sp. The lower bone volume fraction of ROIs might have been weakened in its load-bearing capacity in first place and has ultimately biomechanically collapsed under the load applied on it.¹⁵ Some other studies of the spinal vertebrae micro-CT imaging have shown that within a specimen, these ROIs exhibiting different micro-architecture such as lower bone volume fraction, represented weak points of the structure.¹⁶ Wilke *et al.* studied cervical and lumbar spine vertebrae and showed that the bone volume fraction decreased in female subjects, whereas it was constant in male subjects. The results of this study may help to improve the understanding of pathophysiological changes in the facet joints. Such results could be of value for understanding back pain and its

treatment.¹⁷ Those studies similar to the odontoids, we also calculated the differences in ROIs in the micro-structure but with different parts of the odontoid. In the ROI of the odontoid marrow cavity, the bone volume fraction from parts I had values that were statistically significantly different from those in part IV. We therefore supposed that the rod-like appearance in part IV might be related to the different outcomes in the other parts. Thus, part IV of the odontoid exhibited particularity. This finding is consistent with the results of our micro-CT observation that trabecular bone in part IV comprised a low rod-like structure, whereas there was a more plate-like (than rod-like) structure in the other parts. We thought that type II fractures occur more frequently in part IV of the odontoid because it is the region that exhibits micro-architectural weak points (Fig. 3).

This similarity suggests that the characteristics is occurring in ossification centers of the odontoid. Development of the axis involves ossification of four ossification centers consisting of the vertebral body and the odontoid. The odontoid process fuses to the vertebral body at 3–6 years of age. As even normal odontoid ossification centers may not be completely fused until young adolescence, however, normal areas of incomplete fusion may be mistaken for fractures.¹⁸ We also noted, with micro-CT, that the ossification center formed a trabecular cavity in one of the specimens. The micro-architecture of the ossification center of the odontoid was thus markedly altered compared with normal trabeculae bone (Fig. 4). The ossification center was interspersed with areas devoid of the trabecular cavity that had lower bone volume fractions and thus represented weak points in the structure. Because of an absence of the range of completed trabeculae due to resorption in the ossification center, the base of the

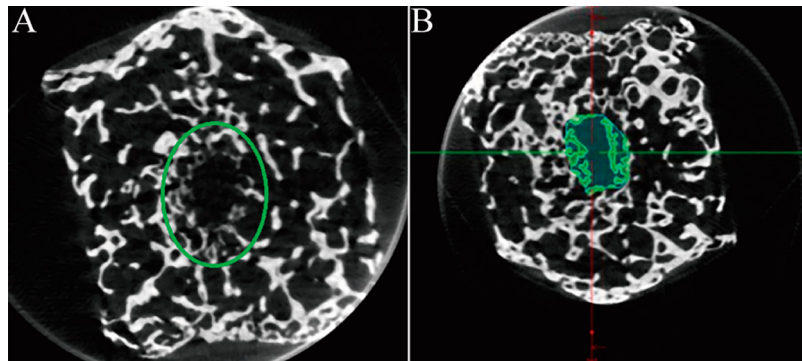


Figure 4 Cross section of the ossification center in the base of the odontoid shows the locations of the region of interest (green region).

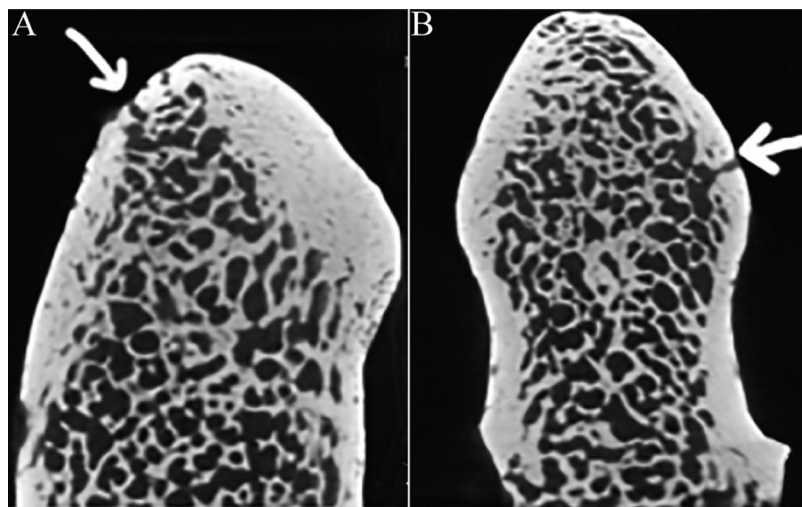


Figure 5 Nutrient foramina were discovered in the sagittal (A) and frontal (B) sections.

odontoid-responsible for its load-bearing capacity—might thus have been weakened.

The base and ossification center of the odontoid had lower bone volume fractions because it is the region that exhibits micro-architectural weak points. We thought that these anatomical specificity may be the important mechanism leading to type II fractures. We surmised that type II fractures that occur at the base of the odontoid junction were more likely because the radial rod-like trabeculae act as load-bearing pillars for transferring forces between the plate-like trabeculae running parallel to the articular surfaces. When the energy is converged and transmitted to the weakest trabecular bone and the tear occurs first. The energy is transmitted along the torn trabecular bone and the bone ultimately fractures under the load applied to it. Factors influencing connectivity in the normal odontoid should be further explored.¹⁹

The present study is limited by its small sample size. However, all the trabecular areas within the ROIs in the four parts of the odontoid that were evaluated

exhibited similar morphology. Also, the statistically significant differences were similar to those reported in other studies.

Our study analyzed the whole odontoid with its nutrient foramina. By capturing the entire 3D micro-architecture of the normal odontoid, we observed the nutrient foramen in its different parts, especially the tip and base of the external odontoid (Fig. 5). The maximum diameter of the nutrient foramen is approximately 0.5 mm. The nutrient foramen into the subchondral bone, connected with internal layers of rod-like trabeculae is rich, allowing good fracture healing. Without quantitating their internal architecture and internal morphology, we believe that it is feasible to use micro-CT as a new research tool to study blood vessels supplying the tissues around bones.

Conclusion

Micro-CT scanning provides a means to study, visualize, and characterize quantitatively the internal micro-architecture of the odontoid, contributing to a better

understanding of the anatomical changes that occur. Because of the high-resolution images produced by micro-CT, visualizing and charting the 3D micro-architecture of the odontoid also enables biomechanical computer simulation studies, such as those using finite element analysis. It also allows investigation of the load-bearing function and its micro-architecture. Biomechanical tests and clinical studies associated with the technique are currently being undertaken.^{20,21}

Disclaimer statements

Contributors None.

Funding This study was supported by the Natural Science Foundation of China [grant numbers 81560348 and 81660358].

Declaration of interest None.

Conflicts of interest Authors have no conflict of interests to declare.

References

- Ryan MD, Henderson JJ. The epidemiology of fractures and fracture-dislocations of the cervical spine. *Injury* 1992;23(1):38–40.
- Smith HE, Kerr SM, Fehlings MG, Chapman J, Maltenfort M, Zavlasky J, *et al.* Trends in epidemiology and management of type II odontoid fractures: 20-year experience at a model system spine injury tertiary referral center. *J Spinal Disord Tech* 2010;23(8):501–5.
- Shamji MF, Alotaibi N, Ghare A, Fehlings MG. Chronic hypertrophic nonunion of the Type II odontoid fracture causing cervical myelopathy: case report and review of literature. *Surg Neurol Int* 2016;7(Suppl 3):S53–6.
- A MS, V TS, B DS. Cruciate paralysis in a 20-year-old male with an undisplaced type III odontoid fracture. *J Orthop Case Rep* 2016;6(2):40–2.
- Patel A, Zakaria R, Al-Mahfoudh R, Clark S, Barrett C, Sarsam Z, *et al.* Conservative management of type II and III odontoid fractures in the elderly at a regional spine centre: a prospective and retrospective cohort study. *Br J Neurosurg* 2015;29(2):249–53.
- Ritman EL. Current status of developments and applications of micro-CT. *Annu Rev Biomed Eng* 2011;13:531–52.
- Perilli E, Parkinson IH, Reynolds KJ. Micro-CT examination of human bone: from biopsies towards the entire organ. *Ann Ist Super Sanita* 2012;48(1):75–82.
- Tassani S, Perilli E. On local micro-architecture analysis of trabecular bone in three dimensions. *Int Orthop* 2013;37(8):1645–6.
- Zhang ZM, Li ZC, Jiang LS, Jiang SD, Dai LY. Micro-CT and mechanical evaluation of subchondral trabecular bone structure between postmenopausal women with osteoarthritis and osteoporosis. *Osteoporos Int* 2010;21(8):1383–90.
- Hildebrand T, Rüegsegger P. Quantification of bone microarchitecture with the structure model index. *Comput Methods Biomed Biomed Engin* 1997;1(1):15–23.
- Boutroy S, Bouxsein ML, Munoz F, Delmas PD. *In vivo* assessment of trabecular bone microarchitecture by high-resolution peripheral quantitative computed tomography. *J Clin Endocrinol Metab* 2005;90(12):6508–15.
- Anderson LD, D'Alonzo RT. Fractures of the odontoid process of the axis. *J Bone Joint Surg Am* 1974;56(8):1663–74.
- Joaquim AF, Patel AA. Surgical treatment of Type II odontoid fractures: anterior odontoid screw fixation or posterior cervical instrumented fusion? *Neurosurg Focus* 2015;38(4):E11.
- Peyrin F. Evaluation of bone scaffolds by micro-CT. *Osteoporos Int* 2011;22(6):2043–8.
- Low SC, Bain GI, Findlay DM, Eng K, Perilli E. External and internal bone micro-architecture in normal and Kienböck's lunates: a whole-bone micro-computed tomography study. *J Orthop Res* 2014;32(6):826–33.
- Perilli E, Parkinson IH, Truong LH, Chong KC, Fazzalari NL, Osti OL. Modic (endplate) changes in the lumbar spine: bone micro-architecture and remodelling. *Eur Spine J* 2015;24(9):1926–34.
- Wilke HJ, Zanker D, Wolfram U. Internal morphology of human facet joints: comparing cervical and lumbar spine with regard to age, gender and the vertebral core. *J Anat* 2012;220(3):233–41.
- Gornet ME, Kelly MP. Fractures of the axis: a review of pediatric, adult, and geriatric injuries. *Curr Rev Musculoskelet Med* 2016;9(4):505–12.
- Wang J, Zhou B, Liu XS, Fields AJ, Sanyal A, Shi X, *et al.* Trabecular plates and rods determine elastic modulus and yield strength of human trabecular bone. *Bone* 2015;72:71–80.
- Mueller TL, Christen D, Sandercott S, Boyd SK, van Rietbergen B, Eckstein F, *et al.* Computational finite element bone mechanics accurately predicts mechanical competence in the human radius of an elderly population. *Bone* 2011;48(6):1232–8.
- Lee DC, Varela A, Kostenuik PJ, Ominsky MS, Keaveny TM. Finite element analysis of denosumab treatment effects on vertebral strength in ovariectomized cynomolgus monkeys. *J Bone Miner Res* 2016;31(8):1586–95.